A Bacterial Tyrosine Phosphatase Inhibits Plant Pattern Recognition Receptor Activation

Alberto P. Macho,[1*] Benjamin Schwessinger,[1*†] Vardis Ntoukakis,[1*‡] Alexandre Brutus,[2] Cécile Segonzac,[1§] Sonali Roy,[1‖] Yasuhiro Kadota,[1] Man-Ho Oh,[3,4] Jan Sklenar,[1] Paul Derbyshire,[1] Rosa Lozano-Durán,[1] Frederikke Gro Malinovsky,[1¶] Jacqueline Monaghan,[1] Frank L. Menke,[1] Steven C. Huber,[3] Sheng Yang He,[2,5] Cyril Zipfel[1#]

Innate immunity relies on the perception of pathogen-associated molecular patterns (PAMPs) by pattern-recognition receptors (PRRs) located on the host cell's surface. Many plant PRRs are kinases. Here, we report that the *Arabidopsis* receptor kinase EF-TU RECEPTOR (EFR), which perceives the elf18 peptide derived from bacterial elongation factor Tu, is activated upon ligand binding by phosphorylation on its tyrosine residues. Phosphorylation of a single tyrosine residue, Y836, is required for activation of EFR and downstream immunity to the phytopathogenic bacterium *Pseudomonas syringae*. A tyrosine phosphatase, HopAO1, secreted by *P. syringae*, reduces EFR phosphorylation and prevents subsequent immune responses. Thus, host and pathogen compete to take control of PRR tyrosine phosphorylation used to initiate antibacterial immunity.

Many plant pattern recognition receptors (PRRs) are receptor kinases, such as the *Arabidopsis* FLS2 and EFR, which recognize the bacterial pathogen-associated molecular patterns (PAMPs) flagellin (or flg22) and elongation factor Tu (EF-Tu) (or elf18), respectively (*1*). Both FLS2 and EFR belong to the non-RD group of kinases (*2*) and are important for antibacterial immunity (*1*). Ligand binding to FLS2 or EFR induces their association with the receptor kinase BAK1, and reciprocal phosphorylation ensues, which initiates immune signaling (*3*). The exact phosphorylation events occurring within these complexes and their biological roles are, however, still unknown. Plant receptor kinases have features of Ser-Thr kinases (*4*). Although tyrosine (Tyr) phosphorylation of receptor kinases is widely studied in mammals (*5*), little is known about its role in plant signaling. Recent studies revealed the involvement of Tyr phosphorylation in RD kinases signaling such as for the receptor kinases BRI1 and BAK1 during growth and for the cytoplasmic kinase BIK1 in immunity (*6*–*9*). However, nothing is known about the importance of Tyr phosphorylation in non-RD kinases, despite its being the major kinase suclass involved in immune signaling across kingdoms (*2*).

To test the relevance of Tyr phosphorylation for plant innate immunity, we pretreated *Arabidopsis*

[1]The Sainsbury Laboratory, Norwich Research Park, Norwich NR4 7UH, UK. [2]Department of Energy Plant Research Laboratory, Michigan State University, East Lansing, MI 48824, USA. [3]U.S. Department of Agriculture–Agricultural Research Service (USDA-ARS) and Department of Plant Biology, University of Illinois, Urbana, IL 61801, USA. [4]Department of Biological Science, College of Biological Sciences and Biotechnology, Chungnam National University, 305-764 Korea. [5]Howard Hughes Medical Institute, Michigan State University, East Lansing, MI 48824, USA.

*These authors contributed equally to this work.
†Present address: Department of Plant Pathology, College of Agricultural and Environmental Sciences, University of California Davis, Davis, CA 95616, USA.
‡Present address: School of Life Sciences, University of Warwick, Coventry CV4 7AL, UK.
§Present address: Institute of Agriculture and Environment, Massey University Manawatu, Palmerston North 4442, New Zealand.
‖Present address: John Innes Centre, Norwich Research Park, Norwich NR4 7UH, UK.
¶Present address: DNRF Center DynaMo, Department of Plant and Environmental Sciences, University of Copenhagen, 1871 Frederiksberg, Denmark.
#Corresponding author. E-mail: cyril.zipfel@tsl.ac.uk

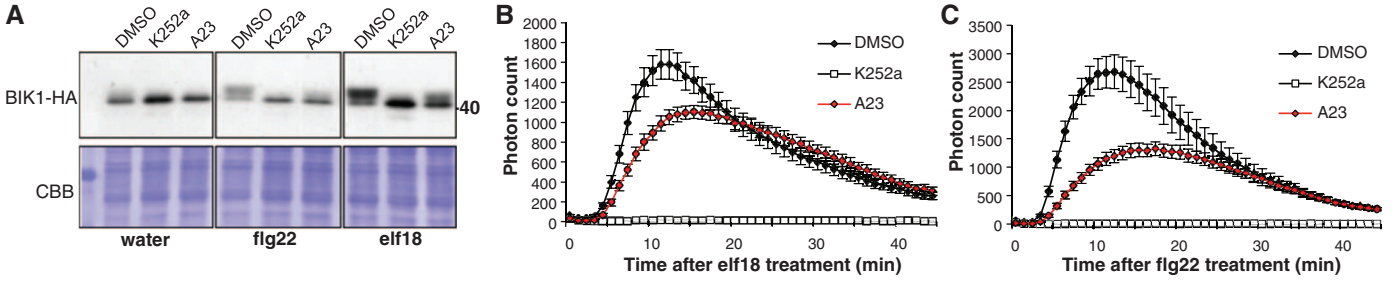

Fig. 1. Tyr phosphorylation is important for PTI responses. One-hour pretreatment of *Arabidopsis* seedlings or leaf disks with 2 μM K252a or 100 μM A23 inhibited immune responses triggered by 100 nM elf18 or flg22. Dimethyl sulfoxide (DMSO) was used as a mock solvent control. (**A**) BIK1 phosphorylation is detected by a mobility-shift of the BIK1-HA (hemagglutinin) band. (**B** and **C**) ROS burst assay. Values are means ± SE, $n = 12$. (**D** and **E**) Quantitative reverse transcription–polymerase chain reaction analyses of PAMP-induced genes. Relative expression levels to the *Ubox* (*At5g15400*) housekeeping gene and normalized to mock-treated seedlings are shown. Values are means ± SE, $n = 3$. Experiments were performed three times with similar results.

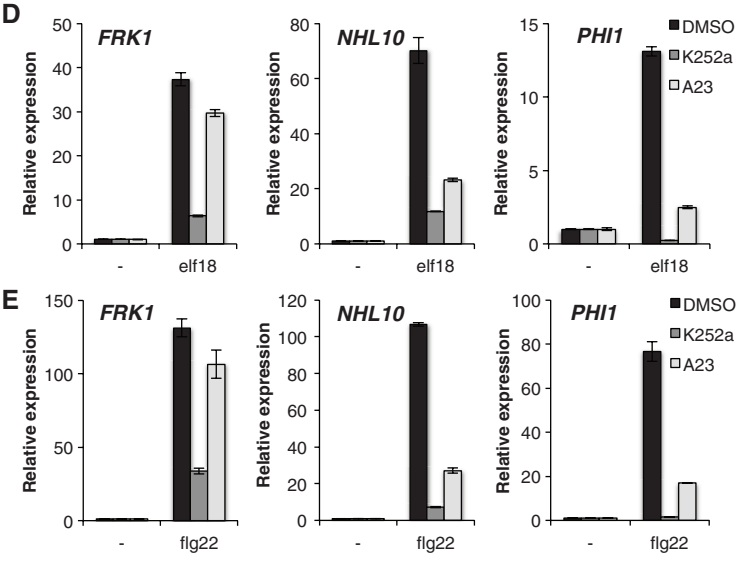

seedlings with the Tyr kinase inhibitor tyrphostin A23 (A23) and assayed typical rapid immune responses. A23 reduced BIK1 phosphorylation and the burst of reactive oxygen species (ROS) normally observed upon PAMP perception (*1*, *10*, *11*) (Fig. 1, A to C). Similarly, A23 reduced the flg22- and elf18-triggered induction of immune-related genes, such as *FRK1*, *NHL10*, and *PHI1* (Fig. 1, D and E). Other Tyr kinase inhibitors, such as tyrphostin A25 and genistein, also reduced elf18-triggered ROS burst (fig. S1). Pretreatment with the general kinase inhibitor K252a suppressed these responses (Fig. 1, A to E). Together, these results suggest that Tyr phosphorylation regulates immune signaling induced by PAMPs.

Next, we tested whether Tyr phosphorylation occurs at the level of non-RD kinase PRRs. We focused on EFR, which is a stronger kinase than

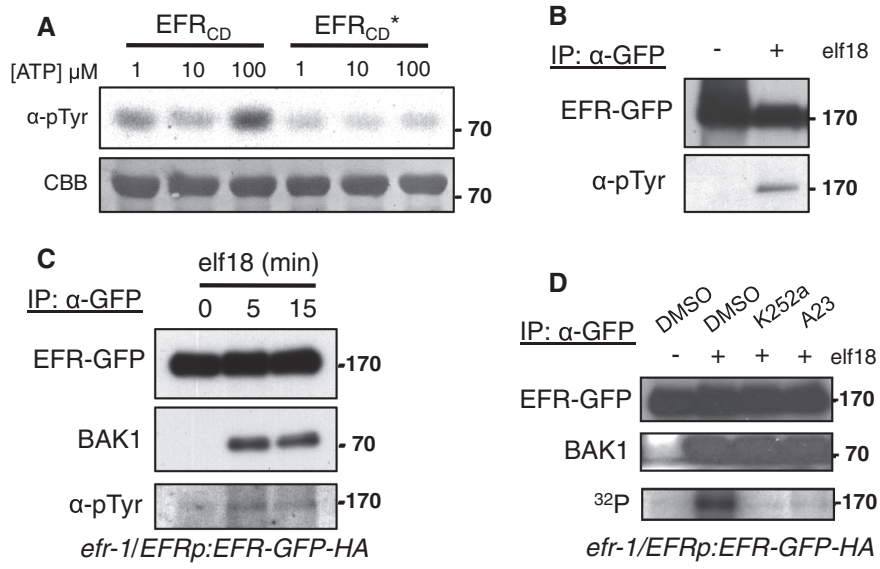

Fig. 2. EFR is phosphorylated on Tyr residues. (A) Recombinant MBP (maltose-binding protein)–EFR phosphorylates on Tyr residues in vitro. EFR*, kinase-dead version (D849N). CD, cytoplasmic domain. **(B)** Tyr phosphorylation on EFR–green fluorescent protein (GFP) immunoprecipitated from *N. benthamiana* after treatment with water (–) or 100 nM elf18 (+) for 10 min. **(C)** Tyr phosphorylation on EFR-GFP immunoprecipitated from *Arabidopsis* seedlings after elicitation with 100 nM elf18. Immunoblots were analyzed with antibodies against phosphorylated tyrosine (anti-pTyr) or anti-GFP. Full anti-pTyr blot is shown in fig. S3. **(D)** Treatment with kinase inhibitors abolishes EFR phosphorylation. *Arabidopsis* seedlings were pretreated for 1 hour with 2 μM K252a or 100 μM A23 before treatment with water (–) or 100 nM elf18 (+) for 10 min. DMSO was used as a mock solvent control. Immunoprecipitated proteins were incubated with [^{32}P]γ-ATP (adenosine 5′-triphosphate). CBB, Coomassie brilliant blue. In vitro phosphorylation was revealed by autoradiography. Experiments were performed three times with similar results.

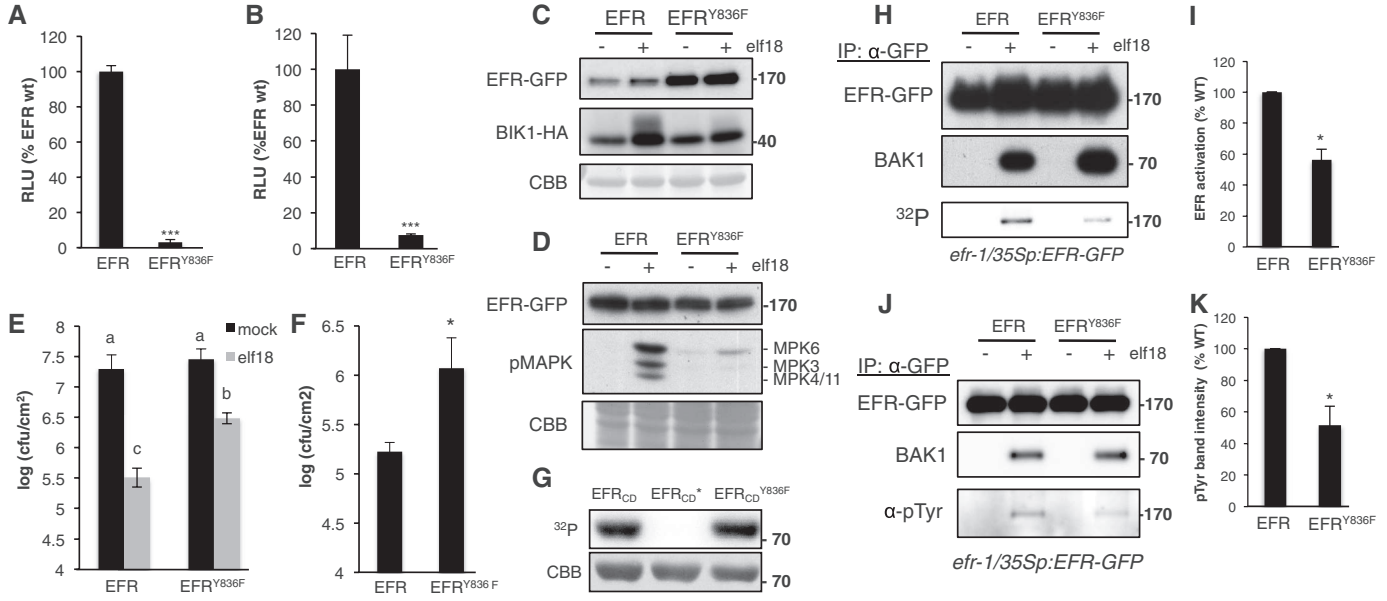

Fig. 3. Y836 is important for EFR function and Tyr phosphorylation. The expression of EFR^{Y836F} compromises elf18-triggered responses in *N. benthamiana* **(A)** or *Arabidopsis efr-1* mutant plants **(B** to **F)**. (A and B) ROS production presented as total photon counts during 40 min after treatment with 100 nM elf18. Values are means ± SE, $n = 12$. RLU, relative luminescence units. (C) *Arabidopsis* EFR-GFP mesophyll protoplasts were transfected with a plasmid expressing *35Sp:BIK1-HA* and treated with water (–) or 100 nM elf18 (+) for 10 min. BIK1 phosphorylation is detected by a mobility shift of the BIK1-HA band. (D) Phosphorylation of MAPKs after treatment with water (–) or 100 nM elf18 (+) for 10 min. (E) Growth of syringe-infiltrated *Pto* DC3000 [10^5 colony-forming units (CFU)/ml)] in leaves pretreated with water (mock) or 1 μM elf18 for 24 hours. Bacterial numbers were determined 2 days after inoculation. Values are mean ± SE, $n = 4$ [one-way analysis of variance (ANOVA); $P < 0.05$]. (F) Growth of surface-inoculated *Pto* DC3000 Δ*avrPto*Δ*avrPtoB* (10^7 CFU/ml), determined 3 days after inoculation. Values are means ± SE, $n = 4$. **(G)** Recombinant MBP-EFR was incubated with [^{32}P]γ-ATP. EFR*, kinase-dead version (D849N). In vitro phosphorylation is revealed by autoradiography. CD, cytoplasmic domain. CBB, Coomassie brilliant blue. **(H)** Activation of EFR-GFP immunoprecipitated from *Arabidopsis* seedlings treated with water (–) or 100 nM elf18 (+) for 10 min. Immunoprecipitated EFR-GFP was incubated with [^{32}P]γ-ATP. In vitro phosphorylation is revealed by autoradiography. **(I)** Mean ± SE of densitometry measurements from three independent replicates of the assay shown in (H). **(J)** Tyr phosphorylation on EFR-GFP immunoprecipitated from *Arabidopsis* seedlings after treatment with water (–) or 100 nM elf18 (+) for 10 min. Immunoblots were analyzed with anti-pTyr, anti-GFP or anti-BAK1. **(K)** Average of densitometry measurements from three independent replicates of the assay shown in (J). Asterisks indicate mean values significantly different from EFR wild type (Student's *t* test; * $P < 0.05$; *** $P < 0.001$). Experiments were performed three times with similar results.

FLS2 (*12*). The EFR cytoplasmic domain was able to phosphorylate on Tyr residues in vitro (Fig. 2A and fig. S2). This phosphorylation was dependent on EFR catalytic activity (Fig. 2A), demonstrating that EFR undergoes autophosphorylation on Tyr residues.

Immunoprecipitation (IP) of EFR transiently expressed in *Nicotiana benthamiana* showed that EFR is phosphorylated on Tyr residues in planta specifically after elicitation with elf18 (Fig. 2B). Similarly, elf18 induced EFR Tyr phosphorylation in *Arabidopsis* (Fig. 2C). Other Tyr-phosphorylated proteins coimmunoprecipitated with EFR, including a band of about 70 kD, which likely corresponds to BAK1 or related proteins (fig. S3). These results demonstrate that EFR undergoes Tyr phosphorylation in vivo in a ligand-dependent manner.

We next tested the role of Tyr phosphorylation in the elf18-induced activation of EFR. To measure EFR phosphorylation, we performed an in vitro kinase assay on EFR immunoprecipitated from *Arabidopsis* seedlings that were or were not pretreated with A23. In this assay, EFR phosphorylation is only detectable after elf18 perception, and this was blocked by A23 treatment (Fig. 2D). The inhibition of EFR phosphorylation was also observed after addition of A23 during the in vitro kinase assay (fig. S4). Together, these results reveal that elf18-dependent Tyr phosphorylation of EFR is essential for the activation of EFR.

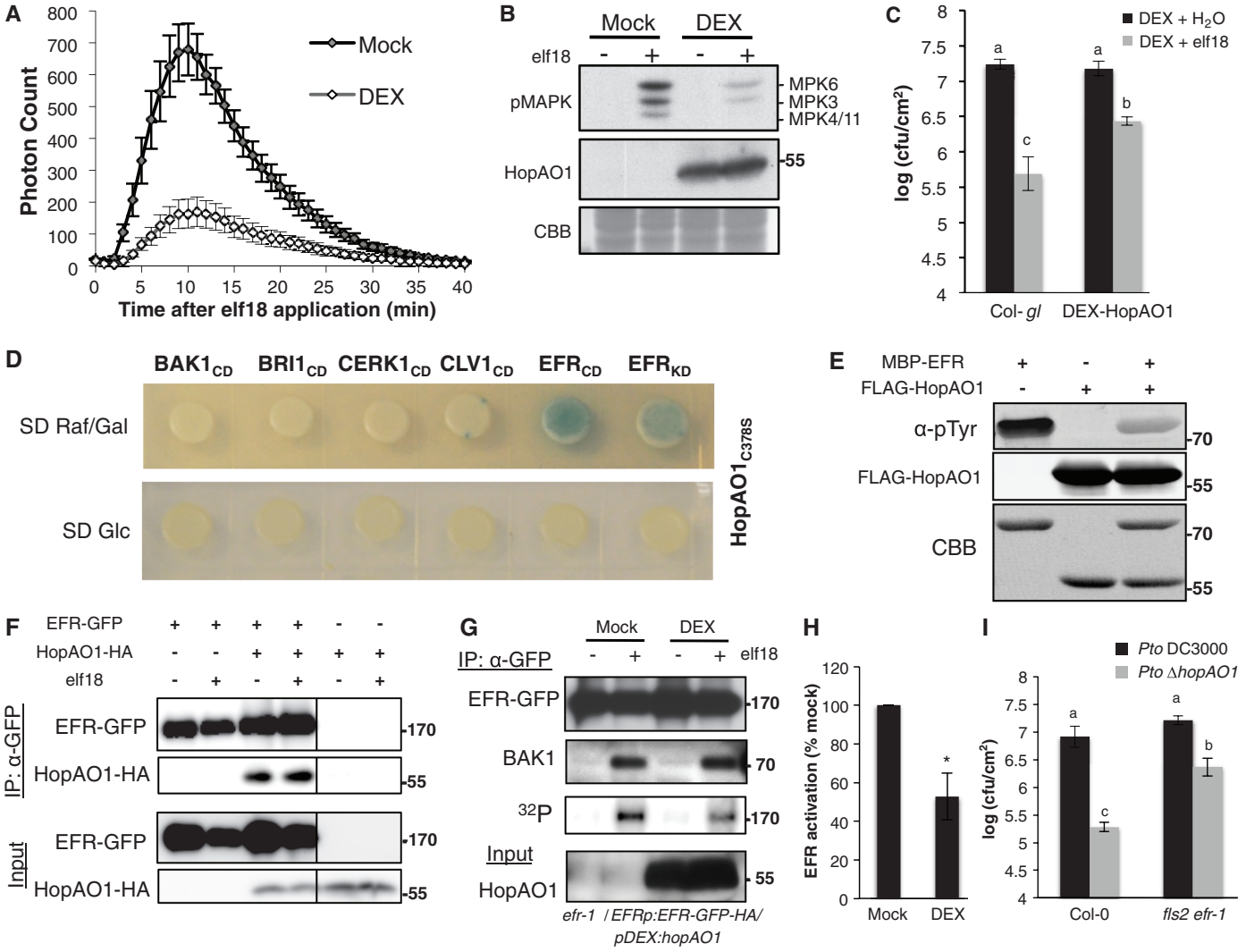

Fig. 4. HopAO1 targets EFR Tyr phosphorylation. Dexamethasone (DEX)–induced expression of HopAO1 in *Arabidopsis* compromises several elf18-induced responses. (**A**) ROS burst measured after a 16 hours' pretreatment with a solvent control (mock) or 30 μM DEX and subsequent treatment with 100 nM elf18. Values are means ± SE, $n = 12$. (**B**) MAPK activation after treatment with water (–) or 100 nM elf18 (+) for 10 min. Seedlings were pretreated for 16 hours with a solvent control (mock) or 30 μM DEX. CBB, Coomassie brilliant blue. (**C**) Growth of syringe-infiltrated *Pto* DC3000 (10^5 CFU/ml) in leaves pretreated with 5 μM DEX for 24 hours, and then treated with water (mock) or 1 μM elf18 for 24 hours. Bacterial numbers were determined 2 days after inoculation. Values are means ± SE, $n = 4$ (one-way ANOVA; $P < 0.05$). (**D**) Yeast-two-hybrid assays to determine the interaction of $HopAO1_{C378S}$ with EFR, BAK1, BRI1, CERK1, and CLV1. CD, cytoplasmic domain; KD, kinase domain. Blue colonies on SD Raf/Gal induction plate indicate positive interaction. (**E**) HopAO1 Tyr phosphatase assay in vitro. Phosphorylated recombinant MBP-EFR was incubated with recombinant FLAG-HopAO1. Immunoblots were analyzed with anti-pTyr or anti-FLAG. CBB, Coomassie brilliant blue. (**F**) Coimmunoprecipitation of EFR-GFP and HopAO1-HA in *N. benthamiana* after treatment with water (–) or 100 nM elf18 (+) for 10 min. Immunoblots were analyzed with anti-GFP or anti-HA. (**G**) EFR activation in *Arabidopsis* seedlings after a 16 hours' pretreatment with a solvent control (mock) or 30 μM DEX and subsequent treatment with water (–) or 100 nM elf18 (+) for 10 min. Immunoprecipitated EFR-GFP was incubated with [^{32}P]γ-ATP. Immunoblots were analyzed with anti-GFP, anti-BAK1, and anti-HopAO1. In vitro phosphorylation is revealed by autoradiography. (**H**) Mean ± SE of densitometry measurements from three independent biological replicates of the assay shown in (G). Asterisk indicates mean values significantly different from mock (Student's *t* test; * $P < 0.05$). (**I**) Growth of syringe-inoculated *Pto* DC3000 or *Pto* DC3000 Δ*hopAO1* (5×10^4 CFU/ml), determined 3 days after inoculation. Values are means ± SE, $n = 4$ (one-way ANOVA; $P < 0.05$). Experiments were performed three times with similar results.

Previously characterized Tyr residues in BRI1 and BAK1 were identified through targeted mutagenesis (*6*, *7*). Therefore, we carried out site-directed mutagenesis to substitute individually each of the 11 Tyr residues present in the EFR cytoplasmic domain with a Phe (F) residue, which lacks the phosphorylatable hydroxyl group. We tested functionality of these variants by expressing them transiently in *N. benthamiana*, which lacks endogenous EFR but otherwise can activate elf18-induced immune responses upon EFR expression (*13*). All variants accumulated to levels similar to that of wild-type EFR (fig. S5). Of the 11 EFR variants tested, only EFR^{Y836F} was fully compromised in mounting an elf18-induced ROS burst (Fig. 3A and fig. S5). Stable transgenic expression of EFR^{Y836F} in *Arabidopsis* did not complement the null *efr-1* mutant phenotype. Lines expressing EFR^{Y836F} were compromised in elf18-triggered ROS burst generation, activation of BIK1, and mitogen-activated protein kinases (MAPKs) (Fig. 3, B to D). The EFR^{Y836F} line was also less resistant to the phytopathogenic bacterium *Pseudomonas syringae* pv. *tomato* (*Pto*) DC3000 in a disease protection assay induced by elf18 pretreatment (Fig. 3E). Additionally, the EFR^{Y836F} line was more susceptible to surface inoculation with the weakly virulent strain *Pto* DC3000 Δ*avrPto* Δ*avrPtoB* (Fig. 3F). These results confirm the importance of EFR^{Y836} in elf18-triggered immunity.

The Y836 residue is located in the kinase subdomain VIa of EFR, is phosphorylated upon elf18 perception in vivo (fig. S6), and is conserved in PRRs and other receptor kinases (fig. S7). EFR^{Y836F} properly accumulates, localizes, and associates with BAK1 in a ligand-dependent manner (Fig. 3 and figs. S5C and S8). EFR^{Y836F} is fully catalytic active and has a kinase activity similar to that of wild-type EFR in vitro (Fig. 3G). The Y839F mutation reduced overall elf18-induced phosphorylation of EFR (Fig. 3, H and I) and Tyr phosphorylation of EFR in vivo (Fig. 3, J and K). Thus, Y836 is a major Tyr phosphorylation site of EFR or is required for the phosphorylation of other EFR Tyr residues. Other Tyr residues, such as Y897, also contribute to the overall ligand-induced Tyr phosphorylation of EFR (fig. S9) but are not as important for downstream signaling (fig. S5). These results provide a mechanistic link between ligand-induced activation of EFR, Tyr phosphorylation (Y836) of the receptor, and the initiation of downstream immune signaling.

Many bacterial pathogens inject effector proteins into the host cell via the type III secretion system to suppress immune processes and components (*14*). One such effector conserved in several *P. syringae* pathovars is HopAO1 (formerly known as HopPtoD2), a protein tyrosine phosphatase (PTP) that contributes to virulence (*15*–*18*). Consistent with previous results (*15*, *17*), we show that inducible expression of HopAO1 in *Arabidopsis* leads to impaired early immune responses, such as elf18-triggered ROS burst and MAPK activation (Fig. 4, A and B), as well as elf18-induced resistance to *Pto* DC3000 (Fig. 4C). Similarly, HopAO1 inhibited flg22-induced ROS burst (fig. S10). Despite its virulence activity and appreciable contribution to overall virulence of *Pto* DC3000, the plant target(s) for HopAO1 is still unknown.

We initially identified the kinase domain of FLS2 as one of the interactors of HopAO1 in a yeast two-hybrid (Y2H) screen using an *Arabidopsis* cDNA library (fig. S10). A catalytically inactive form of HopAO1 ($HopAO1^{C378S}$) (*17*) was used to stabilize potential interactions that otherwise may be transient. Targeted Y2H experiments showed that $HopAO1^{C378S}$ directly interacts with both the kinase and cytoplasmic domains of EFR and FLS2 (Fig. 4D and fig. S10). $HopAO1^{C378S}$ did not interact with the cytoplasmic domain of BAK1, the chitin receptor CERK1, or the receptor kinases BRI1 and CLV1 involved in growth and development, illustrating the specificity of the interactions (Fig. 4D). Consistent with direct interaction, HopAO1 led to a reduced Tyr phosphorylation on EFR in vitro (Fig. 4E). We confirmed this interaction between catalytically active HopAO1 and EFR in planta after transient expression of both proteins in *N. benthamiana* (Fig. 4F). HopAO1 did not interfere with the subcellular localization of EFR (fig. S8) or with its ligand-dependent association with BAK1 (Fig. 4G). These observations indicate that EFR (and potentially FLS2) is a plant target of HopAO1.

Next, we tested whether the interaction of EFR with HopAO1 affects its ligand-induced phosphorylation. Indeed, HopAO1 expression led to a ~50% reduction in the phosphorylation of EFR upon elf18 treatment (Fig. 4, G and H). This reduction was partially dependent on HopAO1 catalytic activity (fig. S11). We could still observe about 20% inhibition of EFR activity by catalytic inactive $HopAO1^{C378S}$. This indicates that the physical interaction of both proteins itself may inhibit EFR phosphorylation. Although we cannot study FLS2 phosphorylation owing to its very low kinase activity, the fact that HopAO1 also interacts with FLS2 and inhibits flg22-induced responses (fig. S10) (*17*) suggests that HopAO1 would also affect its Tyr phosphorylation. In summary, our results indicate that one of the virulence functions of HopAO1 is to target the Tyr phosphorylation of PRRs, such as EFR, thereby inhibiting their ligand-induced activation and downstream immune signaling. Consistent with FLS2 and EFR being important virulence targets for HopAO1 during infection, the virulence defect of *Pto* DC3000 lacking HopAO1 (*Pto* DC3000 Δ*hopAO1*) was alleviated in *fls2 efr-1* double-mutant plants (Fig. 4I).

Our results demonstrate that Tyr phosphorylation drives activation of plant PRRs upon ligand binding. Consistent with its importance in triggering immune responses, this specific posttranslational modification is targeted by the *Pseudomonas* type III–secreted effector HopAO1, which is an active tyrosine phosphatase (*15*, *16*). Animal bacterial pathogens deploy effector proteins that target Tyr phosphorylation, e.g., *Yersinia* YopH or *Salmonella* SptP (*19*), but none of them have been found to target PRRs or associated kinases. The role of Tyr phosphorylation in PRR activation, the important role of HopAO1 in *Pseudomonas* virulence, and the presence of PTP domains in type III–secreted effectors from several bacterial pathogens (*15*, *16*, *18*) illustrate that Tyr phosphorylation is a conserved mechanism important for antibacterial immunity across kingdoms.

References and Notes

1. T. Boller, G. Felix, *Annu. Rev. Plant Biol.* **60**, 379–406 (2009).
2. C. Dardick, B. Schwessinger, P. Ronald, *Curr. Opin. Plant Biol.* **15**, 358–366 (2012).
3. T. W. Liebrand, H. A. van den Burg, M. H. Joosten, *Trends Plant Sci.* **19**, 123–132 (2014).
4. S. H. Shiu, A. B. Bleecker, *Proc. Natl. Acad. Sci. U.S.A.* **98**, 10763–10768 (2001).
5. M. A. Lemmon, J. Schlessinger, *Cell* **141**, 1117–1134 (2010).
6. M. H. Oh *et al.*, *Proc. Natl. Acad. Sci. U.S.A.* **106**, 658–663 (2009).
7. M. H. Oh *et al.*, *Proc. Natl. Acad. Sci. U.S.A.* **107**, 17827–17832 (2010).
8. Y. Jaillais *et al.*, *Genes Dev.* **25**, 232–237 (2011).
9. W. Lin *et al.*, *Proc. Natl. Acad. Sci. U.S.A.* **111**, 3632–3637 (2014).
10. D. Lu *et al.*, *Proc. Natl. Acad. Sci. U.S.A.* **107**, 496–501 (2010).
11. J. Zhang *et al.*, *Cell Host Microbe* **7**, 290–301 (2010).
12. B. Schwessinger *et al.*, *PLOS Genet.* **7**, e1002046 (2011).
13. C. Zipfel *et al.*, *Cell* **125**, 749–760 (2006).
14. F. Feng, J. M. Zhou, *Curr. Opin. Plant Biol.* **15**, 469–476 (2012).
15. J. R. Bretz *et al.*, *Mol. Microbiol.* **49**, 389–400 (2003).
16. A. Espinosa, M. Guo, V. C. Tam, Z. Q. Fu, J. R. Alfano, *Mol. Microbiol.* **49**, 377–387 (2003).
17. W. Underwood, S. Zhang, S. Y. He, *Plant J.* **52**, 658–672 (2007).
18. D. A. Baltrus *et al.*, *PLOS Pathog.* **7**, e1002132 (2011).
19. P. Dean, *FEMS Microbiol. Rev.* **35**, 1100–1125 (2011).

Acknowledgments: This research was funded by the Gatsby Charitable Foundation (C.Z.), the European Research Council (grant "PHOSPHinnATE") (C.Z.), grants BB/E024874/1 (ERA-PG "RLPRLKs") and BB/G024944/1 ERA-PG "Pathonet" from the United Kingdom Biotechnology and Biological Sciences Research Council (C.Z.), grants from U.S. Department of Energy (the Chemical Sciences, Geosciences, and Biosciences Division, Office of Basic Energy Sciences, Office of Science; DE–FG02–91ER20021 for infrastructural support to S.Y.H.), the U.S. National Institutes of Health R01AI060761 (S.Y.H.), the Gordon and Betty Moore Foundation GBMF3037 (S.Y.H.), and grants from the National Science Foundation (MCB-0742411 and 0740211) and USDA-ARS (S.C.H). A.P.M. was supported by a postdoctoral fellowship from the Federation of European Biochemical Societies (FEBS). Y.K. was supported by fellowships from KAKENHI (no. 23580068), the Excellent Young Researcher Overseas Visit Program, and the Uehara memorial foundation. B.S. and S.R. were/are part of the JIC/TSL rotation program. J.M. was supported by a long-term postdoctoral fellowship from the European Molecular Biology Organization. R.L-D. was supported by a postdoctoral fellowship from Fundación Ramón Areces. We thank L. Stransfeld, K. Morehouse, the John Innes Centre horticultural service, and the TSL tissue culture service for technical assistance, and all members of the Zipfel laboratory for discussions and comments. A.P.M., B.S., V.N., A.B., S.C.H., S.Y.H., and C.Z. designed and conceived the experiments. A.P.M., B.S., V.N., A.B., C.S., S.R., Y.K., M.-H.O., R.L.-D., F.G.M., J.M., J.S., and F.L.M. performed the experiments. A.P.M. and C.Z. wrote the manuscript. All authors commented and agreed on the manuscript before submission.

Supplementary Materials

www.sciencemag.org/content/343/6178/1509/suppl/DC1
Materials and Methods
Figs. S1 to S11
Table S1
References (*20*–*24*)

22 November 2013; accepted 28 February 2014
Published online 13 March 2014;
10.1126/science.1248849

A Bacterial Tyrosine Phosphatase Inhibits Plant Pattern Recognition Receptor Activation

Alberto P. Macho, Benjamin Schwessinger, Vardis Ntoukakis, Alexandre Brutus, Cécile Segonzac, Sonali Roy, Yasuhiro Kadota, Man-Ho Oh, Jan Sklenar, Paul Derbyshire, Rosa Lozano-Durán, Frederikke Gro Malinovsky, Jacqueline Monaghan, Frank L. Menke, Steven C. Huber, Sheng Yang He and Cyril Zipfel

Science **343** (6178), 1509-1512.
DOI: 10.1126/science.1248849originally published online March 13, 2014

Move and Countermove

Receptors on plant cell surfaces are tuned to recognize molecular patterns associated with pathogenic bacteria. **Macho *et al.*** (p. 1509; published online 13 March) found that activation of one of these receptors in *Arabidopsis* results in phosphorylation of a specific tyrosine residue, which in turn triggers the plant's immune response to the phytopathogen *Pseudomonas syringae. P. syringae* counters by secreting a specifically targeted phosphatase, thus stalling the plant's immune response.